Anisotropic inversion of MCSEM data based on the integral equation method

Alexander Gribenko and Michael S. Zhdanov, University of Utah

SUMMARY

Marine controlled-source electromagnetic (MCSEM) surveys have become an important part of offshore hydrocarbon (HC) exploration. Marine sediments may exhibit strong anisotropy of electrical conductivity. Ignoring anisotropy may lead to erroneous interpretation of MCSEM data. This paper introduces a 3D inversion of MCSEM data for anisotropic distribution of conductivity based on integral formulation of the EM field equations. Simple modification of the Fréchet derivative expression allows inversion for both horizontal and vertical conductivities. This inversion method has been successfully applied to synthetic data computed for a realistic model of the Harding field.

INTRODUCTION

Marine controlled-source electromagnetic (MCSEM) surveys have become intensively used for offshore petroleum exploration (Eidesmo et al., 2002; Carazzone et al., 2005; Hesthammer et al., 2010). Marine sediments may exhibit strong resistivity anisotropy. Ellis et. al. (2010) report ratios of vertical to horizontal resistivities of 5:1 and greater within the shale-dominated units in the North Sea. The particular case of anisotropy considered here is "transverse isotropy". In the case of transverse isotropy there are two distinct values of resistivity - vertical and horizontal.

Several approaches to the inversion of MCSEM data for 3D anisotropic resistivity distribution have been published. Newman et al. (2010) introduced an inversion algorithm based on finite difference (FD) formulation of the EM field and nonlinear conjugate gradient method (CGM). Wiik et al. (2013) presented another method of MCSEM data inversion using the integral equations (IE) method (Hohmann, 1975) of EM field modeling was used by along with the contrast source inversion method (Abubakar and van den Berg, 2002).

This paper presents a method of anisotropic inversion based on IE forward modeling with a contraction operator (Hursán and Zhdanov, 2002) and a regularized conjugate gradient (RCG) inversion algorithm. We present a synthetic model study considering different scenarios of anisotropy distribution within a sea-bottom sedimentary formation, including both overburden and reservoir targets. We have applied the developed anisotropic inversion method to synthetic MCSEM data computer-simulated for the Harding oil and gas field located in the UK sector of the North Sea.

PROBLEM FORMULATION

We consider, first, a typical MCSEM survey consisting of a set of sea-bottom electrical and magnetic receivers and a horizontal electric dipole transmitter towing at some elevation above the sea bottom. The field recorded by the receivers can be represented as a sum of the normal EM field, $\{\mathbf{E}^{norm}, \mathbf{H}^{norm}\}$, generated in the horizontally layered background model formed by the seawater and the sedimentary layers, and an anomalous part, $\{\mathbf{E}^{a}, \mathbf{H}^{a}\}$, related to the conductivity inhomogeneities, $\Delta\sigma$, present in the sea bottom:

$$\mathbf{E} = \mathbf{E}^{norm} + \mathbf{E}^{a}, \ \mathbf{H} = \mathbf{H}^{norm} + \mathbf{H}^{a}. \tag{1}$$

The anomalous electromagnetic field is related to the electric current induced in the inhomogeneity, $\mathbf{j} = \Delta\sigma\mathbf{E}$, according to the following integral formula:

$$\mathbf{E}^{a}\left(\mathbf{r}_j\right) = \int\int\int_D \widehat{\mathbf{G}}_E\left(\mathbf{r}_j \mid \mathbf{r}\right) \cdot \left[\Delta\sigma\left(\mathbf{r}\right)\mathbf{E}\left(\mathbf{r}\right)\right] dv = \mathbf{G}_E\left[\Delta\sigma\mathbf{E}\right], \tag{2}$$

$$\mathbf{H}^{a}\left(\mathbf{r}_j\right) = \int\int\int_D \widehat{\mathbf{G}}_H\left(\mathbf{r}_j \mid \mathbf{r}\right) \cdot \left[\Delta\sigma\left(\mathbf{r}\right)\mathbf{E}\left(\mathbf{r}\right)\right] dv = \mathbf{G}_H\left[\Delta\sigma\mathbf{E}\right], \tag{3}$$

where $\widehat{\mathbf{G}}_E\left(\mathbf{r}_j \mid \mathbf{r}\right)$ and $\widehat{\mathbf{G}}_H\left(\mathbf{r}_j \mid \mathbf{r}\right)$ are the electric and magnetic Green's tensors defined for an unbounded conductive medium with the normal (horizontally layered) conductivity σ_{norm}; $\mathbf{G}_E$ and $\mathbf{G}_H$ are corresponding Green's linear integral operators; and domain D represents a volume with the anomalous conductivity distribution $\sigma(\mathbf{r}) = \sigma_{norm} + \Delta\sigma(\mathbf{r})$, $\mathbf{r} \in D$.

In most general anisotropic case, conductivity distribution is represented by a $3*3$ tensor. The transverse isotropic medium considered here has two nonequal values of conductivity - horizontal σ_h and vertical σ_v. In a case where the vertical coordinate axis coincides with the anisotropy axis of symmetry (vertical) conductivity tensor takes the form:

$$\widehat{\sigma} = \begin{bmatrix} \sigma_h & 0 & 0 \\ 0 & \sigma_h & 0 \\ 0 & 0 & \sigma_v \end{bmatrix}. \tag{4}$$

This results in both σ_{norm} and $\Delta\sigma$ being represented by tensors similar to (4).

We use integral equations (2) and (3) to formulate both the forward and inverse problems of the MCSEM method. Indeed, in short form these equations can be written as:

$$\mathbf{d} = A\left(\Delta\sigma_h, \Delta\sigma_v\right), \tag{5}$$

where A is a forward modeling operator, $\mathbf{d}$ stands for the observed EM data in the sea-bottom receivers, and $\Delta\sigma_h, \Delta\sigma_v$ are vectors formed by the anomalous horizontal and vertical conductivities within the targeted domain.

INVERSE PROBLEM FORMULATION

The inversion is based on minimization of the Tikhonov parametric functional, $P^{\alpha}\left(\Delta\sigma_h, \Delta\sigma_v\right)$ (Tikhonov and Arsenin, 1977; Zhdanov, 2002):

$$P^{\alpha}\left(\Delta\sigma_h, \Delta\sigma_v\right) = \left\|A\left(\Delta\sigma_h, \Delta\sigma_v\right) - \mathbf{d}\right\|^2 + \alpha s\left(\Delta\sigma_h, \Delta\sigma_v\right). \tag{6}$$

DOI http://dx.doi.org/10.1190/segam2014-0245.1

The first term of the parametric functional represents the data misfit, while the second term is the stabilizer. There are two distinct choices of the stabilizer - smoothing and focusing. In a marine sedimentary environment with structures extending horizontally to great distances it is appropriate to use smoothing Occam-type stabilizer (Constable et al., 1987) with smoothness enforced in the horizontal directions only. A focusing type of stabilizer suitable for reservoir-type targets is an MVS stabilizer, it was specially designed to invert for a thin, sub-horizontal structures typical of HC reservoirs (Zhdanov et al., 2007). We apply the regularized conjugate gradient (RCG) algorithm for minimization of the parametric functional $P(\Delta\sigma)$ (Zhdanov, 2002).

In order to apply RCGM method one needs to compute Fréchet derivative of the forward modeling operator. Direct computation of the Fréchet derivative is very time consuming even when the reciprocity principle is utilized. Fréchet derivatives of the EM field components can be computed using the quasi-Born (QB) approximation (Gribenko and Zhdanov, 2007, 2011):

$$\mathbf{F}|_{\Delta\sigma} = \widehat{\mathbf{G}}\mathbf{E}^{(n)} = \begin{bmatrix} G_x^x & G_x^y & G_x^z \\ G_y^x & G_y^y & G_y^z \\ G_z^x & G_z^y & G_z^z \end{bmatrix} \cdot \begin{bmatrix} E_x & 0 & 0 \\ 0 & E_y & 0 \\ 0 & 0 & E_z \end{bmatrix}, \tag{7}$$

where we omit the E and H subscripts for simplicity.

Note that, the electric field $\mathbf{E}^{(n)}$ is computed using the rigorous IE forward modeling method during the rigorous computations of the predicted fields. Therefore, Fréchet derivatives are obtained by direct multiplication, and no extra forward modeling is required. The QB approximation follows directly from expression (2) after applying perturbation with respect to $\Delta\sigma$. Note that, expression (7) was originally derived for an isotropic conductivity distribution, $\Delta\sigma$. In transverse isotropic case this formula can be easily modified. Let us re-write formula (2) in the tensor notations for a transverse isotropic case:

$$\mathbf{E}^a\left(\mathbf{r}_j\right) = \begin{bmatrix} G_x^x & G_x^y & G_x^z \\ G_y^x & G_y^y & G_y^z \\ G_z^x & G_z^y & G_z^z \end{bmatrix} \cdot \begin{bmatrix} \Delta\sigma_h E_x & 0 & 0 \\ 0 & \Delta\sigma_h E_y & 0 \\ 0 & 0 & \Delta\sigma_v E_z \end{bmatrix}. \tag{8}$$

Applying perturbation to both sides of expression (8) with respect to $\Delta\sigma_h$ and $\Delta\sigma_v$ we obtain the following formulas for Fréchet derivatives:

$$\mathbf{F}|_{\Delta\sigma_h} = \begin{bmatrix} G_x^x & G_x^y \\ G_y^x & G_y^y \\ G_z^x & G_z^y \end{bmatrix} \cdot \begin{bmatrix} E_x & 0 \\ 0 & E_y \end{bmatrix}, \tag{9}$$

$$\mathbf{F}|_{\Delta\sigma_v} = \begin{bmatrix} G_x^z \\ G_y^z \\ G_z^z \end{bmatrix} \cdot E_z, \tag{10}$$

where the Fréchet derivatives $\mathbf{F}|_{\Delta\sigma_h}$ and $\mathbf{F}|_{\Delta\sigma_h}$ can be concatenated, allowing solution of the inverse problem (6) for both the horizontal and vertical conductivities, $\Delta\sigma_h$ and $\Delta\sigma_v$, simultaneously.

To further reduce computational resources and computer memory requirements, we apply the moving sensitivity domain approach to the Fréchet derivative calculation (Cox et al., 2011, Gribenko et al., 2010). MCSEM data derivatives are computed and stored within the sensitivity domain calculated for a given receiver and the corresponding transmitter line.

ANISOTROPIC INVERSION OF MCSEM DATA FOR SIMPLIFIED MODEL OF HC RESERVOIR

We consider a simple box reservoir base model to better understand the effects of anisotropy on the MCSEM inversion. In the model, a prismatic $2.5 \times 2 \times 0.2$ km^3 isotropic resistive body represents a reservoir 600 m deep below the sea bottom. The sea-bottom sediments are represented by a conductive isotropic half-space with 1 Ohm-m resistivity. Seawater depth is 1000 m. The survey configuration consists of three receiver profiles 1 km apart. Each profile consists of 7 receivers located every 500 m. Three transmitter lines pass directly above the receiver profiles, 50 m above the sea bottom. The operating frequency is 0.25 Hz. Both in-line and broadside electric field data are considered in the inversion. Figure 1 shows a vertical section and a 3D view of the model. The transmitter lines and receiver locations are also shown in the figure. Figure 2 presents the vertical sections of the con-

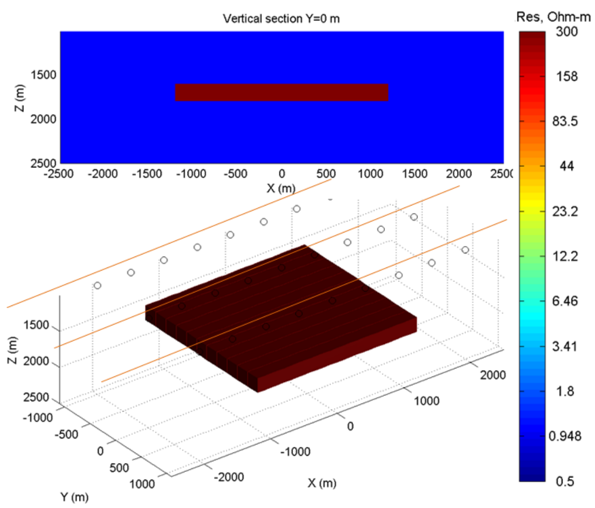

Figure 1: Model 1: A vertical section is shown at the top, a 3D view of the reservoir at the bottom. he receiver locations are represented by circles, and transmitter paths are marked by dashed lines.

ductivity distributions obtained by isotropic and anisotropic inversions. The predicted data computed for the results of both inversions fit the observed data very well with a normalized residual below 1 %. Most of the anomalous resistivity appears in the vertical conductivity for the anisotropic inversion, which indicates that the MCSEM data were less sensitive to the horizontal resistivity of thin structures. This confirms the findings of other researchers (e.g., Ramananjaona et al., 2011, Brown et al., 2012). In the next model we considered the same isotropic reservoir as in model 1, but we added an anisotropic layer on the top of the reservoir, representing an overburden. The survey configuration remained the same. The horizontal resistiv-

DOI http://dx.doi.org/10.1190/segam2014-0245.1

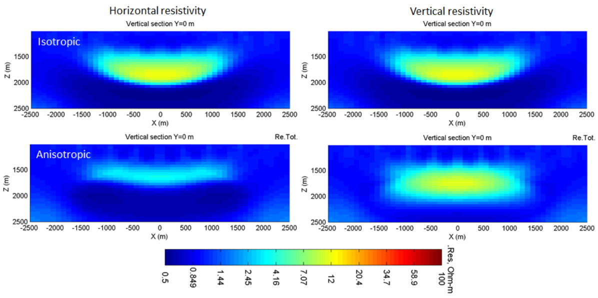

Figure 2: Vertical sections of the resistivity distributions obtained by isotropic (top) and anisotropic (bottom) inversions of model 1 data. Horizontal resistivity is shown in the right panels, vertical in the left. Note the resistivity scale difference with figure 1.

ity of the overburden is 0.5 Ohm-m and the vertical resistivity is 2 Ohm-m. The 3D views and vertical sections of Model 2 are shown in Figure 3. We run inversion of Model 2 data in

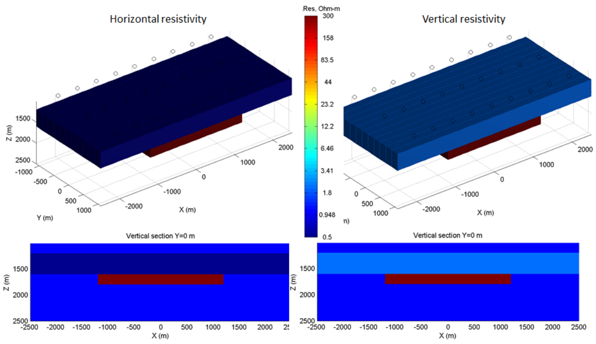

Figure 3: Model 2 - isotropic reservoir with anisotropic overburden. 3D view of the anomalies are shown in the top panels, vertical sections - bottom. Left panels represent horizontal resistivity, right panels - vertical.

two stages. In the first stage we have applied 1D anisotropic inversion in order to estimate the background resistivity distribution. On the second step we run isotropic and anisotropic inversions using the anisotropic background resistivity obtained by 1D inversion. Figure 4 shows the resistivity distributions obtained by these inversions. The two models are equivalent, since they fit the data equally well to less then 1% error. As in the case of Model 1, most of the anomalous resistivity appears in the vertical conductivity for the anisotropic inversion, which indicates again that the MCSEM data were less sensitive to the horizontal resistivity of the thin structures.

INVERSION OF COMPUTER SIMULATED MCSEM DATA FOR HARDING OIL AND GAS FIELD

We have applied the developed anisotropic inversion method to synthetic MCSEM data computer simulated for the Harding oil and gas field located in the UK sector of the North Sea,

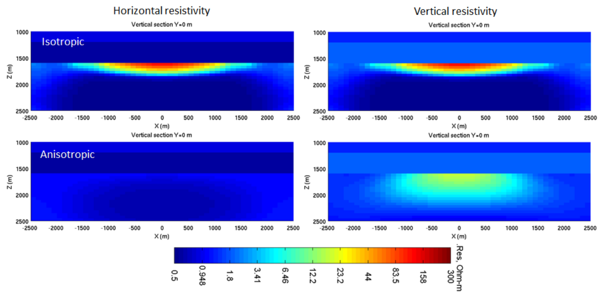

Figure 4: Vertical sections of the resistivity distributions obtained by isotropic (top) and anisotropic (bottom) inversions of model 3 data assuming anisotropic layered background model. The left panels show horizontal resistivity, the right panels present the vertical resistivity.

about 320 km northeast of Aberdeen. The field has a high-net-to-gross, high-quality, Eocene Balder sandstone reservoir about 1,700 m below the seafloor in a 110 m water column.

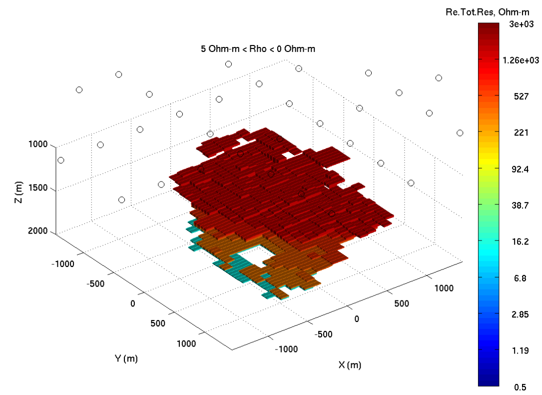

Figure 5: 3D view of the Harding reservoir model. Receivers are shown by circles.

The Harding Central porosity and fluid saturation models were obtained from history matched reservoir simulations constructed from production data, well logs, and 3D seismic interpretations (Ziolkowski et al., 2010; Zhdanov et al., 2012). The corresponding 3D resistivity model of the reservoir is shown in Figure 5. There are 6 receiver profiles running in both x and y directions with 11 receivers on each profile. Both in-line and broadside data considered in the inversion. Three operating frequencies were modeled - 0.1, 0.25, and 1 Hz. The top of the reservoir is filled with highly resistive gas. The resistivity is decreased with depth as the gas part changes to oil and finally to wet reservoir. Note that the shape of the reservoir was assumed known beforehand, and the inversion was restricted to the reservoir boundaries. The goal of the inversion is to recover resistivity distribution within the reservoir keeping the shape of the reservoir unchanged. We included a 500 m thick anisotropic overburden layer on top of the reservoir and

DOI http://dx.doi.org/10.1190/segam2014-0245.1

assumed otherwise homogeneous 1 Ohm-m half space as our background model.

We ran inversions for isotropic resistivity distribution within the reservoir, but assumed two scenarios. First, the background conductivity was assumed isotropic at 1 Ohm-m. The recovered resistivity distributions are shown in Figure 6 . Obviously, the inversion failed to recover the resistive top of the reservoir transforming it to conductive towards the bottom. The observed data could only be fit to 6% error. In the second scenario we assumed background with known anisotropic overburden. Figure 7 shows vertical and horizontal sections of the inversion result. The transition from the resistive to conductive regions within the reservoir is well recovered. The observed data were fit to less then 1% error.

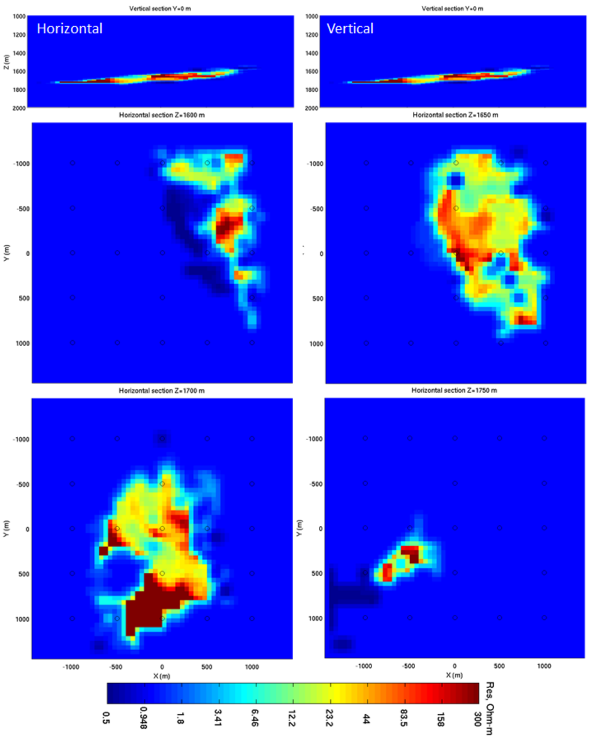

Figure 6: Inversion result of the Harding model data assuming an isotropic background. Top panels: vertical sections of the horizontal (left) and vertical (right) resistivity (same). The middle and bottom panels represent horizontal sections at different depths.

CONCLUSIONS

We have developed a method of 3D inversion of MCSEM data for anisotropic resistivity distribution. Our method is based on an integral equation EM field formulation. The quasi-Born approximation with a moving sensitivity domain approach were used for efficient Fréchet derivative calculation. A simple modification of the Fréchet derivative allowed us to run the inversion for both the horizontal and vertical resistivity distributions.

The model study concurs with published results. The MCSEM data have limited sensitivity to horizontal resistivity of the reservoir targets. Unaccounted anisotropy in the overburden may lead to erroneous MCSEM data interpretation and it may not produce an acceptable data fit. The anisotropic inversion in similar situation may provide more accurate estimation of the target location, but may also produce artifacts. Better data fits may be achieved with the anisotropic inversion. The most efficient way of dealing with the extensive overburdens seems to be an estimation of the horizontally layered anisotropic background structure by 1D inversion, and subsequent 3D isotropic or anisotropic inversions. Modeling of the realistic Harding field data confirms that, a good estimate of overburden resistivity is necessary for accurate recovery of the reservoir resistivity distribution.

ACKNOWLEDGMENTS

The authors acknowledge the support of the University of Utah Consortium for Electromagnetic Modeling and Inversion (CEMI) and TechnoImaging.

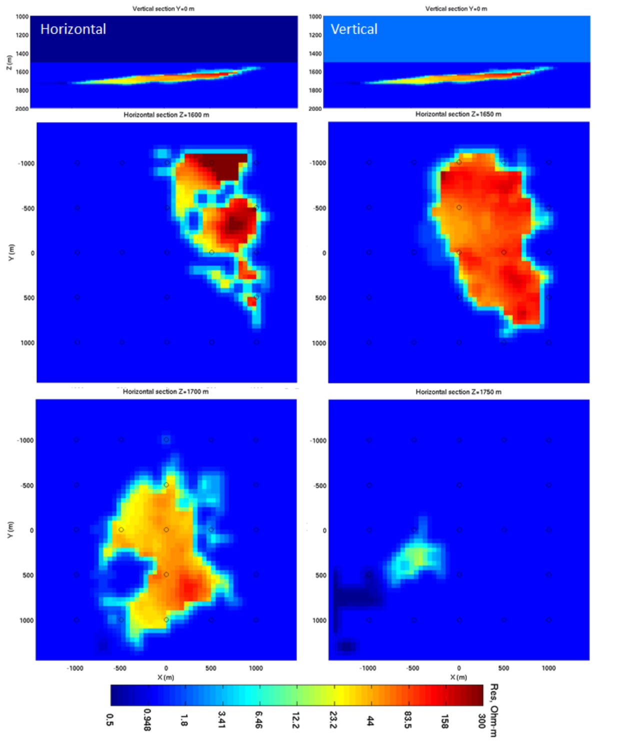

Figure 7: Inversion result of the Harding model data assuming an anisotropic background. Top panels: vertical sections of the horisontal (left) and vertical (right) resistivity (same). The middle and bottom panels represent horizontal sections at different depths.

DOI http://dx.doi.org/10.1190/segam2014-0245.1

http://dx.doi.org/10.1190/segam2014-0245.1

EDITED REFERENCES

Note: This reference list is a copy-edited version of the reference list submitted by the author. Reference lists for the 2014 SEG Technical Program Expanded Abstracts have been copy edited so that references provided with the online metadata for each paper will achieve a high degree of linking to cited sources that appear on the Web.

REFERENCES

Abubakar, A., and P. M. van den Berg, 2002, The contrast source inversion method for location and shape reconstructions: Inverse Problems, **18**, no. 2, 495–510, http://dx.doi.org/10.1088/0266-5611/18/2/313.

Brown, V., M. Hoversten, K. Key, and J. Chen, 2012, Resolution of reservoir scale electrical anisotropy from marine CSEM data: Geophysics, **77**, no. 2, E147–E158, http://dx.doi.org/10.1190/geo2011-0159.1.

Carazzone, J. J., O. M. Burtz, K. E. Green, D. A. Pavlov, and C. Xia, 2005, Three dimensional imaging of marine CSEM data: 75th Annual International Meeting, SEG, Expanded Abstracts, 575–578.

Constable, S. C., R. L. Parker, and C. G. Constable, 1987, Occam's inversion: A practical algorithm for generating smooth models from electromagnetic sounding data: Geophysics, **52**, 289–300, http://dx.doi.org/10.1190/1.1442303.

Cox, L. H., G. A. Wilson, and M. S. Zhdanov, 2010, 3D inversion of airborne electromagnetic data using a moving footprint: Exploration Geophysics, **41**, no. 4, 250–259, http://dx.doi.org/10.1071/EG10003.

Eidesmo, T., S. Ellingsrud, L. M. MacGregor, S. Constable, M. C. Sinha, S. Johansen, F. N. Kong, and H. Westerdahl, 2002, Sea bed logging (SBL), a new method for remote and direct identification of hydrocarbon filled layers in deepwater areas: First Break, **20**, 144–152.

Ellis, M., M. Sinha, and R. Parr, 2010, Role of fine-scale layering and grain alignment in the electrical anisotropy of marine sediments: First Break, **28**, no. 10, 49–57.

Gribenko, A., A. M. Green, M. Cuma, and M. S. Zhdanov, 2010, Efficient 3D inversion of MT data using integral equations method and the receiver footprint approach: Application to the large-scale inversion of the EarthScope MT data: 80th Annual International Meeting, SEG, Expanded Abstracts, 644–649.

Gribenko, A., and M. S. Zhdanov, 2007, Rigorous 3D inversion of marine CSEM data based on the integral equation method: Geophysics, **72**, no. 2, WA73–WA84, http://dx.doi.org/10.1190/1.2435712.

Gribenko, A. V., and M. S. Zhdanov, 2011, Joint 3D inversion of marine CSEM and MT data: 81st Annual International Meeting, SEG, Expanded Abstracts, 552–556.

Hesthammer, J., A. Stefatos, M. Boulaenko, S. Fanavoll, and J. E. Danielsen, 2010, CSEM performance in light of well results: The Leading Edge, **29**, 34–41, http://dx.doi.org/10.1190/1.3284051.

Hohmann, G. W., 1975, Three-dimensional induced polarization and electromagnetic modeling: Geophysics, **40**, 309–324, http://dx.doi.org/10.1190/1.1440527.

Hursán, G., and M. S. Zhdanov, 2002, Contraction integral equation method in three-dimensional electromagnetic modeling: Radio Science, **37**, no. 6, doi: 10.1029/2001RS002513.

Newman, G. A., M. Commer, and J. J. Carazzone, 2010, Imaging CSEM data in the presence of electrical anisotropy: Geophysics, **75**, no. 2, F51–F61, http://dx.doi.org/10.1190/1.3295883.

Ramananjaona, C., L. MacGregor, and D. Andréis, 2011, Sensitivity and inversion of marine electromagnetic data in a vertically anisotropic stratified earth: Geophysical Prospecting, **59**, no. 2, 341–360, http://dx.doi.org/10.1111/j.1365-2478.2010.00919.x.

Tikhonov, A. N., and V. Y. Arsenin, 1977, Solution of ill-posed problems: Winston & Sons.

Wiik, T., K. Hokstad, B. Ursin, and L. Mütschard, 2013, Joint contrast source inversion of marine magnetotelluric and controlled source electromagnetic data: Geophysics, **78**, no. 6, E315–E327, http://dx.doi.org/10.1190/geo2012-0477.1.

Zhdanov, M. S., 2002, Geophysical inverse theory and regularization problems: Elsevier.

Zhdanov, M. S., C. Anderson, M. Endo, L. H. Cox, M. Cuma, N. Black, and A. V. Gribenko, 2012, 3D inversion of towed streamer EM data: A model study of the Harding field with comparison to CSEM: First Break, **30**, 71–74.

Zhdanov, M. S., A. Gribenko, and M. Cuma, 2007, Regularized focusing inversion of marine CSEM data using minimum vertical-support stabilizer: 77th Annual International Meeting, SEG, Expanded Abstracts, 579–583.

Ziolkowski, A., R. Parr, D. Wright, V. Nockles, C. Limond, E. Morris, and J. Linfoot, 2010, Multi-transient electromagnetic repeatability experiment over the North Sea Harding field: Geophysical Prospecting, **58**, 1159–1176.